

# Cilostazol attenuates oxidative stress and apoptosis in the quadriceps muscle of the dystrophic mouse experimental model

Túlio de Almeida Hermes<sup>1,2</sup>  | Rafael Dias Mâncio<sup>1</sup>  | Daniela Sayuri Mizobutti<sup>1</sup> | Aline Barbosa Macedo<sup>1</sup>  | Larissa Akemi Kido<sup>1</sup> | Valéria Helena Alves Cagnon Quitete<sup>1</sup>  | Elaine Minatel<sup>1</sup> 

<sup>1</sup>Department of Structural and Functional Biology, Institute of Biology, State University of Campinas (UNICAMP), São Paulo, Brazil

<sup>2</sup>Departament of Anatomy, Institute of Biomedical Sciences, Federal University of Alfenas (UNIFAL-MG), Alfenas, Brazil

## Correspondence

Túlio de Almeida Hermes,  
Department of Anatomy, Federal University of Alfenas, Unifal-MG, 700 Gabriel Monteiro da Silva, St. Alfenas, Brazil.  
Email: [tulio.hermes@unifal-edu.br](mailto:tulio.hermes@unifal-edu.br) and [tulio.ah13@gmail.com](mailto:tulio.ah13@gmail.com),

## Funding information

Conselho Nacional de Desenvolvimento Científico e Tecnológico; Coordenação de Aperfeiçoamento de Pessoal de Nível Superior; Fundação de Amparo à Pesquisa do Estado de São Paulo, Grant/Award Number: 11/02474-4

## Abstract

Duchenne muscular dystrophy (DMD) is the most severe and frequent form of muscular dystrophy. The mdx mouse is one of the most widely used experimental models to understand aspects of the biology of dystrophic skeletal muscles and the mechanisms of DMD. Oxidative stress and apoptosis are present in early stages of the disease in mdx mice. The high production of reactive oxygen species (ROS) causes activation of apoptotic death regulatory proteins due to DNA damage and breakdown of nuclear and mitochondrial membranes. The quadriceps (QUA) muscle of the mdx mouse is a good tool to study oxidative events. Previous studies have demonstrated that cilostazol exerts an anti-oxidant effect by decreasing the production of reactive oxygen species (ROS). The present study aimed to evaluate the ability of cilostazol to modulate oxidative stress and apoptosis in the QUA muscle of mdx mice. Fourteen-day-old mdx mice received cilostazol or saline for 14 days. C57BL/10 mice were used as a control. In the QUA muscle of mdx mice, cilostazol treatment decreased ROS production (−74%), the number of lipofuscin granules (−47%), lipid peroxidation (−11%), and the number of apoptotic cells (−66%). Thus cilostazol showed anti-oxidant and anti-apoptotic action in the QUA muscle of mdx mice.

## KEYWORDS

apoptosis, cilostazol, Duchenne muscular dystrophy, mdx mice, oxidative stress

## 1 | INTRODUCTION

Duchenne muscular dystrophy (DMD) is the most severe and frequent form of muscular dystrophy, affecting 1 in 5000 male births.<sup>1</sup> DMD is an X-linked disorder characterized by a progressive and irreversible degenerative of the skeletal muscles<sup>2</sup> due to the fragility of

the muscle fibre owing to the absence of the dystrophin protein and alteration of the dystrophin-glycoprotein complex (DGC).<sup>3,4</sup>

The mdx mouse (X chromosome-linked muscular dystrophy) is one of the most widely used experimental models to understand aspects of the biology of dystrophic skeletal muscles and the mechanisms of DMD.<sup>5</sup> This model is

deficient in dystrophin production, but its phenotype is milder than DMD.<sup>6</sup> Therapeutic interventions initiated in the pre-necrotic stage<sup>7,8</sup> provide a good window of observation and prevention of events triggered by the absence of dystrophin in the animal, such as exacerbation of inflammation, extensive myonecrosis, and oxidative stress.<sup>9</sup>

Oxidative stress is present in the primary stages of muscle degeneration in dystrophic muscle.<sup>9</sup> Studies have shown a significant increase in the production of reactive oxygen species (ROS), sarcolemma lipid peroxidation, and/or imbalance in antioxidant enzymes in early stages of the disease in mdx mice and in patients with dystrophy.<sup>10,11</sup> Increases in oxidative indicators have been observed even before 4 weeks of age in mdx mice and 2 years of age in patients with dystrophy.<sup>10</sup> The high ROS production in dystrophic muscle is a result of intracellular accumulation of calcium ions and their abnormal uptake by mitochondria.<sup>12</sup>

The reduced form of molecular oxygen, the superoxide anion ( $O_2^{\bullet-}$ ), is a prominent ROS, formed from incomplete transfer of electrons from complex I to complex III of the mitochondrial electron transport chain.<sup>13</sup>  $O_2^{\bullet-}$  can undergo dismutation spontaneously or by the enzymatic action of superoxide dismutase (SOD), leading to the formation of hydrogen peroxide ( $H_2O_2$ ).<sup>14</sup> From the oxidation of transition metals that are freely available in the cell, such as iron,  $H_2O_2$  can produce the hydroxyl radical ( $OH^{\bullet}$ ).<sup>15</sup> This species causes damage to DNA, RNA, proteins, lipids, and nuclear and mitochondrial membranes. In DNA, it affects both nitrogenous bases and deoxyribose by abstracting one of the hydrogen atoms and usually leads to DNA strand breakage. When produced close to a membrane, lipids can be oxidized and initiate a chain reaction with free radicals leading to membrane lipid peroxidation, producing the by-product 4-hydroxy-2-nonenal (4-HNE).<sup>15,16</sup> DNA damage causes activation of apoptotic death regulatory proteins as well as the transcription factors necessary for the expression of pro- and anti-apoptotic genes.<sup>17,18</sup> Anti-oxidant enzymes (SOD, catalase [CAT], and glutathione peroxidase [GPx]) act by reducing the rate of free radical generation and/or by eliminating them.<sup>19</sup> Normally, these enzymes act efficiently and manage to control and restore the redox balance; however, under exhaustion conditions (as in mdx mice) a state of oxidative stress is created.<sup>20</sup>

Opening of the mitochondrial permeability transition pore (MPTP) requires pro-apoptotic proteins, such as Bax, binding to specific sites in the mitochondrial membrane, voltage-gated ion channels, and other proteins.<sup>21,22</sup> The MPTP directly impairs mitochondrial selectivity and calcium homeostasis and allows the release of cytochrome c into the cytoplasm; this molecule is the main inducer of the apoptotic cascade via caspase activation.<sup>21–24</sup> Although necrosis is the most relevant type of cell death in dystrophic muscle tissue, the initial signs of histologically detectable muscle cell death in the mdx mouse show that

myonuclear apoptosis precedes necrosis.<sup>25,26</sup> Moorwood and Barton<sup>27</sup> demonstrated that caspase-12 ablation preserves muscle function and reduces degeneration in the long digital extensor muscle of mdx mice and related these effects to reduced apoptosis.

Type II muscle fibres (fast fibres) are preferentially affected in DMD.<sup>28</sup> Thus, the diaphragm (DIA) and muscles of the limbs, such as the quadriceps (QUA), are more susceptible to damage, presenting a greater inflammatory infiltrate, a large number of fibres with a central nucleus, and extensive myonecrosis.<sup>29–32</sup> This factor is involved in determining the muscles and experimental strategies involving the mdx mouse. In addition, the QUA muscle of the mdx mouse is a good tool to study oxidative events. This muscle presents important changes in the activity of all enzymes linked to the Krebs cycle and to the mitochondrial respiratory chain, as well as a reduction in maximal respiratory activity and a reduction in inner mitochondrial membrane proteins.<sup>33,34</sup> Furthermore, Hughes et al.<sup>35</sup> demonstrated that maximum  $H_2O_2$  emission in the QUA muscle is dependent on mitochondrial density or the abundance of respiratory chain complexes, unlike the DIA and gastrocnemius muscle, and is the only muscle to exhibit decreased mitochondrial calcium retention capacity, which indicates increased sensitivity to MPTP opening.

Cilostazol (6-[4-(1-cyclohexyl-1H-tetrazol-5-yl)butoxy]-3,4-dihydro-2(1H)-quinolinone) is a potent antiplatelet, antithrombotic, and vasodilatory agent that acts by inhibiting the enzyme phosphodiesterase type 3A (PDE-3) and thus increasing the levels of 3',5'-cyclic adenosine monophosphate (cAMP), present in smooth muscle cells.<sup>36</sup> However, more and more studies have demonstrated the anti-oxidant effect (radical scavenger) of cilostazol to decrease  $O_2^{\bullet-}$  and thus eliminate  $OH^{\bullet}$ .<sup>37–39</sup> Cilostazol also demonstrated this effect in the DIA of mdx mouse, including reducing inflammatory and degenerative indicators and improving muscle strength.<sup>40</sup>

Based on the above information, evaluation of the anti-oxidant effect of cilostazol in dystrophic tissue can be better understood when applied to the alterations in the structural and functional patterns of the mitochondria of the QUA muscle in the mdx mouse. Therefore, the present study aimed to evaluate the ability of cilostazol administration to modulate the high ROS production, oxidative stress, and programmed cell death in the QUA muscle of mdx mice.

## 2 | MATERIALS AND METHODS

### 2.1 | Animals

Male and female C57BL/10 (C57BL/10ScCr/PasUnib) and mdx mice (C57BL/10-Dmdmdx/PasUnib) were used in this study. Care of the mice was based on the guidelines of the

Brazilian College for Animal Experimentation (COBEA) and institutional guidelines. Cilostazol treatment was started on postnatal day 14 prior to muscle degeneration-regeneration cycles.<sup>41</sup> The institutional Ethics Committee on the Use of Animals (CEUA) of State University of Campinas (UNICAMP; process #3115-1) approved the research protocol.

## 2.2 | Cilostazol administration

For 14 days, 14-day-old mdx mice (mdxC group,  $n = 25$ ) received 100 mg cilostazol/kg body weight daily (Eurofarma<sup>®</sup>) diluted in 0.05 ml of saline via oral gavage. Control 14-day-old mdx mice (mdxS group,  $n = 16$ ) received only saline. The animals were weighed daily to adjust the drug dose. C57BL/10 mice (Ctrl group) that did not receive treatment and used as control. The person doing the analysis was not blinded as to the treatment that each mouse had received.

## 2.3 | Histopathological analysis ( $n = 5$ )

After the 14-day treatments, the animals were anaesthetised intraperitoneally with a lethal dose of 2% xylazine hydrochloride solution (Vyrbaxyl, Virbac) and ketamine hydrochloride (Francotar, Virbac) (1:1 at a dose of 0.1 ml/30 g body weight) and perfused with phosphate-buffered saline (PBS). The QUA muscle was removed, frozen in isopentane cooled to  $-159^{\circ}\text{C}$  by liquid nitrogen and stored in a biofreezer at  $-70^{\circ}\text{C}$ . The muscles were sectioned with a cryostat kept at  $-23^{\circ}\text{C}$ ; 8- $\mu\text{m}$ -thick transverse sections were collected on a slide. Six slides with about 12 sections each were obtained from each animal and used in the analyses described below.

### 2.3.1 | Lipofuscin analysis

The number of autofluorescent lipofuscin granules was quantified. The muscle samples ( $n = 5$  per group) were analysed using unfixed 8  $\mu\text{m}$ -thick transverse sections of the QUA muscle. Quantification was performed with an inverted fluorescence microscope (Nikon, Eclipse TS100/TS100F) using the NIS-elements AR Advances Research software in each cross-section (4–5 sections per muscle).

### 2.3.2 | Dihydroethidium (DHE) reaction analysis

To determine ROS (specifically  $\text{O}_2^{\bullet-}$ ), the QUA muscle cross-sections were incubated with DHE.<sup>42</sup> The QUA sections were incubated with 5  $\mu\text{l}$  of the dihydroethidium (DHE) in PBS, at  $37^{\circ}\text{C}$  for 30 min, washed with PBS,

and mounted in DABCO (mounting medium for fluorescence microscopy; Sigma). DHE staining appears as a bright red emission when viewed with a fluorescence microscope. The fluorescence area (%) of the DHE was obtained (pixel limit: 70–255 wavelength).

### 2.3.3 | Terminal deoxynucleotidyl transferase dUTP nick end labeling (TUNEL) assay to detect apoptotic cells

Apoptotic cells were detected with the TUNEL method (Dead End<sup>™</sup> Fluorometric TUNEL System, Promega), according to the manufacturer's instructions. Apoptotic cells were identified and captured by an inverted fluorescence microscope (Nikon<sup>®</sup>, Eclipse TS100/TS100F). Ten random fields for each animal were captured at 40 $\times$  magnification. The quantification was determined by the number of TUNEL-positive fluorescent nuclei divided by the total number of DAPI-counterstained nuclei. The result is expressed as the relative frequency of positive fluorescent labeling in all experimental groups.<sup>43</sup>

## 2.4 | Western blot analysis ( $n = 6$ )

After euthanasia of the animals as described above, the left and right QUA muscles were collected, pooled and homogenized (1% Triton, 10 mM sodium pyrophosphate, 100 mM NaF, 10  $\mu\text{g}/\text{ml}$  aprotinin, 1 mM phenylmethylsulfonyl fluoride, and 0.25 mM  $\text{Na}_3\text{VO}_4$ ). Cell detritus was removed by centrifugation at 13,800 g for 20 min at  $4^{\circ}\text{C}$  and the supernatant was subjected to sodium dodecyl sulfate-polyacrylamide gel electrophoresis (SDS-PAGE) gel electrophoresis. The Bradford method was used to determine the total protein content. Total protein from cell lysate (30  $\mu\text{g}$ ) was stacked on 6%–15% SDS-polyacrylamide gels.

The proteins were transferred from gels to nitrocellulose membranes by electrophoresis (Mini Trans-Blot electrophoretic transfer cell, Bio-Rad). Membranes were incubated with the appropriate primary antibodies overnight at  $4^{\circ}\text{C}$  with gentle shaking: goat polyclonal anti-4-HNE (Santa Cruz Biotechnology), mouse monoclonal anti-anti-catalase (Sigma-Aldrich), rabbit anti-SOD-2 (Sigma-Aldrich), and rabbit polyclonal anti-glyceraldehyde-3-phosphate dehydrogenase (GAPDH, Santa Cruz Biotechnology). The membranes were then incubated with the appropriate secondary antibody, anti-mouse or anti-rabbit IgG conjugated to peroxidase (KPL), for 2 h at room temperature. Membranes were washed three times for 10 min each with Tris buffered saline-Tween 20 (TBST) after both incubations. GAPDH was used as a control protein loading. Protein bands were visualized using the Clarity Western ECL Substrate (Bio-Rad).

GENETOOLS software (SynGene) was used for band intensities quantification.

## 2.5 | Biochemical analysis ( $n = 5$ )

After euthanasia, the left and right QUA muscles were removed, pooled and homogenized in a tissue homogenizer with 1 ml of PBS, immediately immersed in liquid nitrogen, and stored in a biofreezer ( $-70^{\circ}\text{C}$ ). Subsequently, the samples were used to quantify enzymatic activities and the reduced glutathione (GSH) content.

### 2.5.1 | SOD1 activity

SOD1 activity was evaluated based on reducing nitroblue tetrazolium using a xanthine-xanthine oxidase system, that is, superoxide generation, which can be measured by the absorbance at 420 nm.<sup>44</sup> The results are shown as SOD units per mg of protein.

### 2.5.2 | GSH content

The total GSH content was analysed with Ellman's reaction using 5'5'-dithio-bis-2-nitrobenzoic acid (DTNB) as per Anderson.<sup>45</sup> The yellow colour intensity was read at 412 nm. The results are shown as nmol per mg of protein.

### 2.5.3 | GPx activity

Quantification of the GPx activity was based on the decrease in absorbance at 365 nm induced by 0.25 mM  $\text{H}_2\text{O}_2$  with GSH (10 mM), NADPH, (4 mM), and 1 U of glutathione reductase (GR).<sup>46</sup> The results are shown as nmol per min per mg of protein.

### 2.5.4 | GR activity

GR activity was quantified as described by Carlberg and Mannervick,<sup>47</sup> based on the decrease in absorbance at 340 nm induced by oxidized glutathione (GSSG) with NADPH in phosphate buffer (pH 7.8). Absorbance changes were read from 1 to 10 min. The results are shown as nmol per min per mg of protein.

## 2.6 | Statistical analysis

All the results are presented as the mean  $\pm$  standard deviation (SD). Comparisons were carried out using one-way

analysis of variance (ANOVA), followed by Tukey's post hoc *t*-test.  $p \leq 0.05$  was considered to be statistically significant.

## 3 | RESULTS

### 3.1 | Effect of cilostazol on oxidative stress in the QUA muscle

There was an intense area of DHE fluorescence, characterizing a significant increase in the production of ROS, in the mdxS group compared with the Ctrl group (Figure 1). After the experimental treatments, there was a reduction in ROS production in the mdxC group (about 56%) relative to the mdxS group (Figure 1).

The mdxS group showed a significant increase in the number of lipofuscin granules in the QUA muscle compared with the Ctrl group, characterizing the high chronic oxidative pattern in dystrophic animals (Figure 1). The mdxC group had a significantly reduced number of lipofuscin granules (about 47%) in the QUA muscle compared with the mdxS group (Figure 1).

4-HNE increased in the QUA muscle of the mdxS group (Figures 1, S1). Cilostazol treatment significantly reduced 4-HNE levels in the mdxC group (about 11%) compared with the mdxS group (Figures 1, S1).

### 3.2 | Effect of cilostazol on the antioxidant activity in the QUA muscle

CAT increased in the treated and untreated mdx groups compared with the Ctrl group, but there was not a significant difference. The SOD2 levels were similar in all experimental groups (Figure 2).

The GSH levels were increased in the QUA muscle of the mdxS and mdxC groups compared with the Ctrl group (Figure 2). There were no difference in SOD1 between the mdxS and mdxC groups (Figure 2).

There was a significant difference in GR and GPx activity: They increased significantly in the mdxS and mdxC groups compared with the the Ctrl group (Figure 2).

### 3.3 | Effect of cilostazol on apoptosis in the QUA muscle

There was an accumulation of cells undergoing apoptosis in the mdxS group compared with the Ctrl group (Figure 3). The mdxC group had a significantly reduced number of apoptotic cells (about 71%) compared with the mdxS group. This reduction in the number of apoptotic cells observed in both experimental treatments indicates that the drug's effects are associated with oxidative stress (Figure 3).

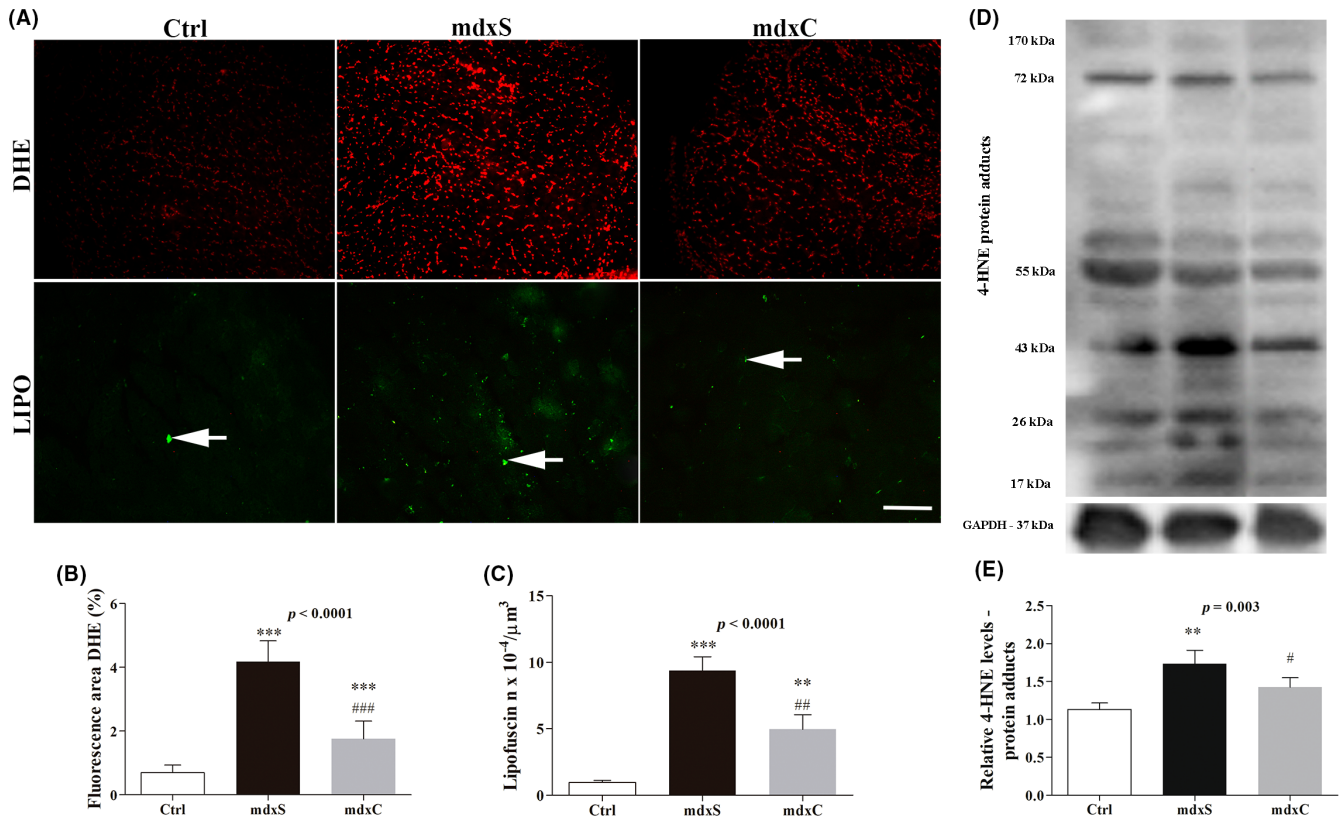


**FIGURE 1** (A) Quadriceps (QUA) cross-sections showing dihydroethidium (DHE,  $n = 5$  each group) fluorescence and autofluorescent lipofuscin granules (LIPO, white arrow,  $n = 5$  each group) in C57BL/10 mice (Ctrl), saline-treated mdx mice (mdxS), and cilostazol-treated mdx mice (mdxC). (B) The graph shows the DHE staining area (%) in the Ctrl, mdxS, and mdxC groups. (C) The graph shows the number of lipofuscin granules  $\times 10^{-4}/\mu\text{m}^3$  in the Ctrl, mdxS, and mdxC groups. (D) Western blotting analysis ( $n = 6$  each group) of 4-hydroxynonenal (4-HNE)-protein adducts. Bands corresponding to protein adducts formed by the reaction of 4-HNE with nucleophilic protein residues (top panel) and glyceraldehyde-3-phosphate dehydrogenase (GAPDH; used as a loading control) (bottom row) are shown. (E) The graphs show protein levels in the crude extracts of QUA muscle from the Ctrl, mdxS and mdxC groups. All values are expressed as mean  $\pm$  standard deviation (SD). \*\* $p \leq 0.001$  compared with the Ctrl group, \*\*\* $p \leq 0.0001$  compared with the Ctrl group (Student's  $t$ -test). # $p \leq 0.05$  compared with the mdxS group, ## $p \leq 0.001$  compared with the mdxS group, ### $p \leq 0.0001$  compared with the mdxS group (Student's  $t$ -test). The scale bar is 100  $\mu\text{m}$ .

## 4 | DISCUSSION

In the present study, the administration of cilostazol significantly reduced oxidative stress markers (DHE [measure of ROS], lipofuscin granules, and 4-HNE protein adducts) and the number of apoptotic cells in the QUA muscle of mdx mice. The interaction between these two events highlights the metabolic complications of dystrophic muscle fibres, given that apoptosis induced by ROS overproduction is one of the results of mitochondrial dysfunction.<sup>48</sup> Consistent with these findings, exercised mdx mice treated with tempol, a potent anti-oxidant, showed increased levels of mitochondrial biogenesis regulators.<sup>49</sup> We chose to investigate the interaction of cilostazol against oxidative stress and apoptosis in the QUA muscle of mdx mice because it presents metabolic alterations that have been strongly established in the literature.<sup>33–35</sup> Although the TUNEL method is often considered the gold standard for

the detection of apoptosis in situ due to its high sensitivity, the false positivity of TUNEL against programmed necrotic cell death (necroptotic cells) should be considered in the present study.<sup>50,51</sup> Considering that the basal lamina was not identified in the present method, it is important to make it clear that TUNEL+ nuclei may be satellite cells or myonuclei, but may also be fibrocytes, fibroadipogenic precursor cells (FAPs) and/or macrophages, that are present in dystrophic muscle.<sup>52,53</sup>

Oxidative stress and apoptosis are present in early stages of the disease in mdx mice.<sup>9,10,25,26</sup> The use of anti-oxidants such as *N*-acetylcysteine, tempol, green tea, or ascorbic acid in mdx mice <30 days of age demonstrates beneficial results in the disease phenotype by decreasing muscle weakness, inflammation, and dystrophic tissue degeneration.<sup>54–58</sup> We demonstrated previously that cilostazol administration attenuated markers of oxidative stress (DHE and 4-HNE) and inflammation in the DIA of mdx mice associated with

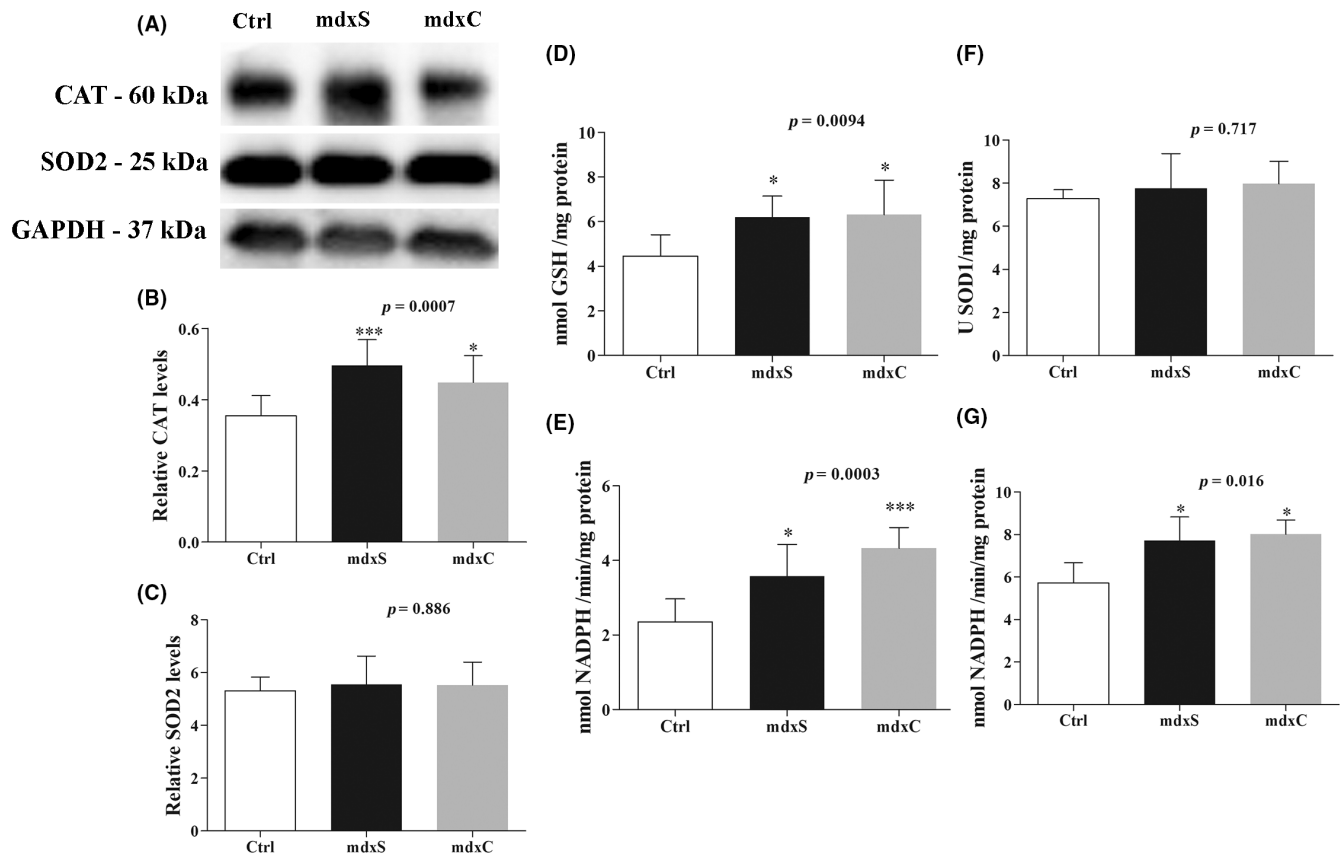


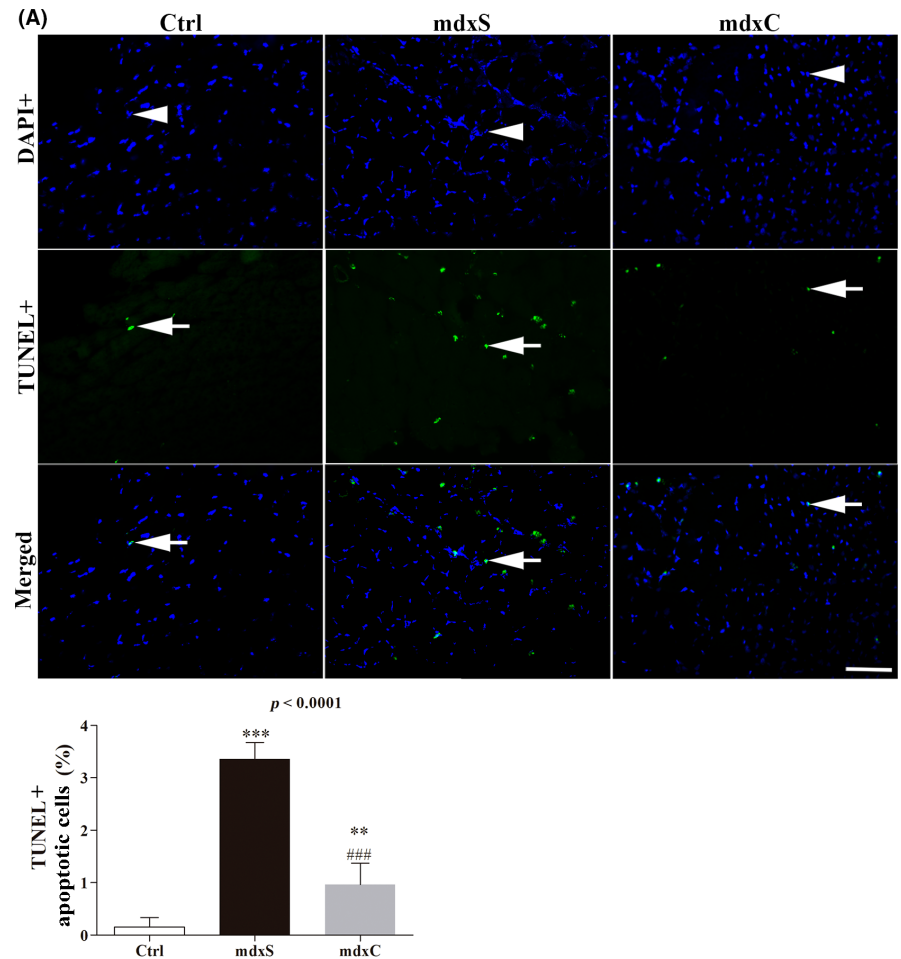
**FIGURE 2** (A) Western blotting analysis ( $n = 6$  each group) of catalase (CAT) and superoxide dismutase 2 (SOD2) content in the quadriceps (QUA) from C57BL/10 mice (Ctrl), saline-treated mdx mice (mdxS), and cilostazol-treated mdx mice (mdxC). Bands corresponding to proteins (top and middle row) and glyceraldehyde-3-phosphate dehydrogenase (GAPDH; used as a loading control) (bottom row) are shown. The graphs show: protein levels of (B) CAT and (C) SOD2; biochemical analysis ( $n = 5$  each group) of content of (D) reduced glutathione (GSH) and (F) superoxide dismutase 1 (SOD1), and activity of (E) glutathione peroxidase (GPx) and (G) glutathione reductase (GR) in the crude extracts of QUA muscle from the Ctrl, mdxS, and mdxC groups. All values are expressed as mean  $\pm$  standard deviation (SD). \* $p \leq 0.05$  compared with the Ctrl group, \*\*\* $p \leq 0.0001$  compared with the Ctrl group (Student's  $t$ -test).

preservation of muscle strength.<sup>40</sup> In cardiomyocytes from rats under oxidative stress, cilostazol prevented mitochondrial dysfunction by attenuating cardiac mitochondrial edema, ROS production, and changes in the mitochondrial membrane potential of cardiac cells.<sup>59</sup> Comparatively, the anti-oxidant effect of cilostazol is as effective as other classic anti-oxidant compounds already tested in the mdx model in terms of improving the dystrophic phenotype. Tempol, a potent anti-oxidant, has been shown to reduce myonecrosis and inflammation, associated with a reduction in oxidative stress markers such as DHE, lipofuscin granule count, and 4-HNE in the diaphragm muscle of mdx mice.<sup>54,55,60</sup> The use of the anti-oxidant N-acetylcysteine had a beneficial effect on dystrophic muscle tissue by reducing indicators of oxidative stress, inflammation and fibrosis.<sup>42,61,62</sup> Similarly, green tea extract as well as its isolated compounds decreased muscle necrosis in mdx mice via antioxidant pathways.<sup>63–65</sup> These studies support our results in terms of attenuation of oxidative stress markers in the QUA muscle of mdx mice; however, the exact mechanism is unclear.

Dystrophic muscles present functional ischemia generated by low production of nitric oxide (NO) in skeletal and endothelial muscle cells.<sup>66–70</sup> Cilostazol has an effect on vascular smooth muscle cells, which from both the increase in cAMP, and from the inhibition of PDE-3, is able to promote the relaxation of the endothelium, and as a consequence, vasodilation.<sup>36</sup> With the lack of blood flow and oxygen supply, there is a decrease in ATP production, which induces anaerobic metabolism, producing a lower level of anti-oxidant agents in cells.<sup>71</sup> Therefore, it is possible that vasodilation contributes, in part, to the improvement of the redox state of dystrophic muscle. However, in the present study, changes in anti-oxidant enzymes and GSH content in the QUA muscle of mdx mice were not observed after a 14-day treatment with cilostazol.

The beneficial effects of cilostazol, such as antiplatelet and anti-inflammatory properties, are attributed to activation of AMP-activated protein kinase (AMPK).<sup>72–74</sup> AMPK plays an important role in regulating the energy balance of eukaryotic cells: It monitors changes in the ATP level,

**FIGURE 3** (A) Quadriceps (QUA) cross-sections showing apoptotic cells (terminal deoxynucleotidyl transferase dUTP nick end labeling [TUNEL] positive, white arrow; DAPI positive, white arrowhead.  $n = 5$  each group) in C57BL/10 mice (Ctrl), saline-treated mdx mice (mdxS), and cilostazol-treated mdx mice (mdxC). (B) The graph shows the relative frequency of positive fluorescent labeling to apoptotic cells (%) in the Ctrl, mdxS, and mdxC groups. (C) All values are expressed as the mean  $\pm$  standard deviation (SD). \* $p \leq 0.05$  compared with the Ctrl group, \*\*\* $p \leq 0.0001$  compared with the Ctrl group (Student *t*-test). ### $p \leq 0.0001$  compared with the mdxS group (Student *t*-test). The scale bar is 50  $\mu\text{m}$ .



increasing the rate of ATP production pathways and/or decreasing the rate of ATP utilization pathways, as well as regulating the biogenesis and degradation of mitochondria.<sup>75,76</sup> In skeletal muscle, AMPK transmits a part of the signal by which muscle contraction increases glucose uptake into the cell.<sup>77</sup> Studies have described the radical scavenger action and apoptotic cell death of cilostazol by AMPK activation and its effect on energy homeostasis and mitochondrial protection.<sup>37,78</sup> Supporting this, our results showed those effects without influencing the anti-oxidant system, consistent with previous observation in the DIA.<sup>40</sup> Studies indicate an increase in GPx and SOD-1 in the mdx mouse, but in the pre-necrotic period of muscle degeneration.<sup>79</sup> In agreement with our results, cilostazol administration significantly reduced malondialdehyde, an indicator of lipid peroxidation, but did not significantly alter the activity of the anti-oxidant enzymes SOD and CAT (catalase) in an experimental model of aortic occlusion.<sup>37</sup>

Chronic AMPK stimulation in mdx mice has produced beneficial phenotypic changes in dystrophic skeletal muscle, such as a shift from type II (fast and glycolytic) myofibers to type I (slow and oxidative), accompanied by increased utrophin expression and improved stability of

the sarcolemma.<sup>80</sup> Abou-Samra et al.<sup>81</sup> administered adiponectin as an AMPK activator and observed a reduction in inflammation, oxidative stress, and muscle damage, associated with increased expression of myogenic differentiation markers, as well as upregulation of utrophin in the tibialis anterior muscle of mdx mice, results that are consistent with our findings. Similarly, studies have shown that suppression of apoptosis is related to activation of the AMPK pathway.<sup>82–84</sup> AMPK pathway activation via cilostazol protected rat hepatocytes against alcohol-induced apoptosis.<sup>85</sup> Therefore, based on our findings and other studies, we suggest that the anti-oxidant action of cilostazol and the prevention of apoptosis in the QUA muscle observed in the present study may be related to the activation of AMPK and to regulatory pathways of mitochondrial biogenesis. Future studies are needed to test this hypothesis.

Based on the results, it was possible to verify a potent anti-oxidant action of cilostazol by reducing markers of oxidative stress and prevention of apoptosis in the QUA muscle of mdx mice, which was not associated with endogenous enzymatic anti-oxidant regulation. The attenuation of oxidative stress and programmed cell death in the QUA muscle evidences a possible regulation of the

metabolic pattern of the dystrophic cell; however, future studies are still necessary to investigate this relationship. Cilostazol represents a potential pharmacological strategy for the treatment of DMD.

## AUTHORS CONTRIBUTIONS

TAH: Project administration, Animals treatment, Formal analysis, Data curation, Methodology and investigation, Writing—original draft. RDM: Data curation, Methodology and investigation. DSM: Methodology and investigation. ABM: Methodology and investigation. LAK: Methodology and investigation. VACQ: Resources, Validation, Review, Methodology, Writing—original draft. EM: Conceptualization, Project administration, Funding acquisition, Resources, Validation, Review, Methodology, Writing—original draft.

## ACKNOWLEDGEMENTS

This work was supported by Fundação de Amparo à Pesquisa do Estado de São Paulo (FAPESP, grant 11/02474-4) and by Coordenação de Aperfeiçoamento de Pessoal de Nível Superior (CAPES-PROEX). TAH was the recipient of a CAPES fellowship, ABM was the recipient of a CNPq fellowship, and RDM and LAK were recipients of FAPESP fellowships (#14/01970-6; #13/01294-8).

## CONFLICT OF INTEREST

The authors declare that they have no competing interests.

## ORCID

Túlio de Almeida Hermes  <https://orcid.org/0000-0003-2937-3890>

Rafael Dias Mâncio  <https://orcid.org/0000-0002-6299-187X>

Aline Barbosa Macedo  <https://orcid.org/0000-0002-4156-9370>

Valéria Helena Alves Cagnon Quitete  <https://orcid.org/0000-0001-5331-7376>

Elaine Minatel  <https://orcid.org/0000-0001-9863-0761>

## REFERENCES

- Mendell JR, Shilling C, Leslie ND, et al. Evidence-based path to newborn screening for Duchenne muscular dystrophy. *Ann Neurol*. 2012;71(3):304-313.
- Schmalbruch H. Skeletal muscle fibers of newborn rats are coupled by gap junctions. *Dev Biol*. 1982;91(2):485-490.
- Ibraghimov-Beskrovnaya O, Ervasti JM, Leveille CJ, Slaughter CA, Sernett SW, Campbell KP. Primary structure of dystrophin-associated glycoproteins linking dystrophin to the extracellular matrix. *Nature*. 1992;355(6362):696-702.
- Matsumura K, Burghes AH, Mora M, et al. Immunohistochemical analysis of dystrophin-associated proteins in Becker/Duchenne muscular dystrophy with huge in-frame deletions in the NH2-terminal and rod domains of dystrophin. *J Clin Invest*. 1994;93(1):99-105.
- Bulfield G, Siller WG, Wight PA, Moore KJ. X chromosome-linked muscular dystrophy (mdx) in the mouse. *Proc Natl Acad Sci USA*. 1984;81(4):1189-1192.
- Chen CN, Graber TG, Bratten WM, Ferrington DA, Thompson LV. Immunoproteasome in animal models of Duchenne muscular dystrophy. *J Muscle Res Cell Motil*. 2014;35(2):191-201.
- Minatel E, Neto HS, Marques MJ. Acetylcholine receptor distribution and synapse elimination at the developing neuromuscular junction of mdx mice. *Muscle Nerve*. 2003;28(5):561-569.
- Shavlakadze T, White J, Hoh JF, Rosenthal N, Grounds MD. Targeted expression of insulin-like growth factor-I reduces early myofiber necrosis in dystrophic mdx mice. *Mol Ther*. 2004;10(5):829-843.
- Whitehead NP, Yeung EW, Allen DG. Muscle damage in mdx (dystrophic) mice: role of calcium and reactive oxygen species. *Clin Exp Pharmacol Physiol*. 2006;33(7):657-662.
- Nakae Y, Stoward PJ, Kashiyama T, et al. Early onset of lipofuscin accumulation in dystrophin-deficient skeletal muscles of DMD patients and mdx mice. *J Mol Histol*. 2004;35(5):489-499.
- Rodriguez MC, Tarnopolsky MA. Patients with dystrophinopathy show evidence of increased oxidative stress. *Free Radic Biol Med*. 2003;34(9):1217-1220.
- Brookes PS, Yoon Y, Robotham JL, Anders MW, Sheu SS. Calcium, ATP, and ROS: a mitochondrial love-hate triangle. *Am J Physiol Cell Physiol*. 2004;287(4):C817-C833.
- Trachootham D, Lu W, Ogasawara MA, Nilsa RD, Huang P. Redox regulation of cell survival. *Antioxid Redox Signal*. 2008;10(8):1343-1374.
- Fridovich I. Superoxide radical and superoxide dismutases. *Annu Rev Biochem*. 1995;64:97-112.
- Barreiros ALBS, David JM. Estresse Oxidativo: Relação entre geração de espécies reativas e defesa do organismo. *Quim Nova*. 2006;29:113-123.
- Forman HJ, Zhang H, Rinna A. Glutathione: overview of its protective roles, measurement, and biosynthesis. *Mol Aspects Med*. 2009;30(1-2):1-12.
- Primeau AJ, Adhietty PJ, Hood DA. Apoptosis in heart and skeletal muscle. *Can J Appl Physiol*. 2002;27(4):349-395.
- Ji LL. Antioxidant signaling in skeletal muscle: a brief review. *Exp Gerontol*. 2007;42(7):582-593.
- deZwart LL, Meerman JH, Commandeur JN, Vermeulen NP. Biomarkers of free radical damage applications in experimental animals and in humans. *Free Radic Biol Med*. 1999;26(1-2):202-226.
- Vasconcelos SML, Goulart MOF, Moura JBF, Manfredini V, Benfato MS, Kubota LT. Espécies reativas de oxigênio e de nitrogênio, antioxidantes e marcadores de dano oxidativo em sangue humano: principais métodos analíticos para sua determinação. *Química Nova*. 2007;30:1323-1338.
- Adhietty PJ, Hood DA. Mechanisms of apoptosis in skeletal muscle. *Basic Appl Ecol*. 2003;13:171-179.
- Baines CP, Kaiser RA, Purcell NH, et al. Loss of cyclophilin D reveals a critical role for mitochondrial permeability transition in cell death. *Nature*. 2005;434(7033):658-662.
- Nakagawa T, Shimizu S, Watanabe T, et al. Cyclophilin D-dependent mitochondrial permeability transition regulates some necrotic but not apoptotic cell death. *Nature*. 2005;434(7033):652-658.
- Schinzel AC, Takeuchi O, Huang Z, et al. Cyclophilin D is a component of mitochondrial permeability transition and

- mediates neuronal cell death after focal cerebral ischemia. *Proc Natl Acad Sci USA*. 2005;102(34):12005-12010.
25. Tidball JG, Albrecht DE, Lokensgard BE, Spencer MJ. Apoptosis precedes necrosis of dystrophin-deficient muscle. *J Cell Sci*. 1995;108(Pt 6):2197-2204.
  26. Spencer MJ, Walsh CM, Dorshkind KA, Rodriguez EM, Tidball JG. Myonuclear apoptosis in dystrophic mdx muscle occurs by perforin-mediated cytotoxicity. *J Clin Invest*. 1997;99(11):2745-2751.
  27. Moorwood C, Barton ER. Caspase-12 ablation preserves muscle function in the mdx mouse. *Hum Mol Genet*. 2014;23(20):5325-5341.
  28. Webster C, Silberstein L, Hays AP, Blau HM. Fast muscle fibers are preferentially affected in Duchenne muscular dystrophy. *Cell*. 1988;52(4):503-513.
  29. Kim JH, Lawler JM. Amplification of proinflammatory phenotype, damage, and weakness by oxidative stress in the diaphragm muscle of mdx mice. *Free Radic Biol Med*. 2012;52(9):1597-1606.
  30. Grounds MD, Radley HG, Lynch GS, Nagaraju K, De Luca A. Towards developing standard operating procedures for pre-clinical testing in the mdx mouse model of Duchenne muscular dystrophy. *Neurobiol Dis*. 2008;31(1):1-19.
  31. Haslett JN, Kang PB, Han M, et al. The influence of muscle type and dystrophin deficiency on murine expression profiles. *Mamm Genome*. 2005;16(10):739-748.
  32. Schneider JS, Shanmugam M, Gonzalez JP, et al. Increased sarcolipin expression and decreased sarco(endo)plasmic reticulum Ca<sup>2+</sup> uptake in skeletal muscles of mouse models of Duchenne muscular dystrophy. *J Muscle Res Cell Motil*. 2013;34(5-6):349-356.
  33. Kuznetsov AV, Winkler K, Wiedemann FR, vonBossanyi P, Dietzmann K, Kunz WS. Impaired mitochondrial oxidative phosphorylation in skeletal muscle of the dystrophin-deficient mdx mouse. *Mol Cell Biochem*. 1998;183(1-2):87-96.
  34. Comim CM, Hoepers A, Ventura L, et al. Activity of Krebs cycle enzymes in mdx mice. *Muscle Nerve*. 2016;53(1):91-95.
  35. Hughes MC, Ramos SV, Turnbull PC, et al. Early myopathy in Duchenne muscular dystrophy is associated with elevated mitochondrial H<sub>2</sub>O<sub>2</sub> emission during impaired oxidative phosphorylation. *J Cachexia Sarcopenia Muscle*. 2019;10(3):643-661.
  36. Schror K. The pharmacology of cilostazol. *Diabetes Obes Metab*. 2002;4(Suppl 2):S14-S19.
  37. Kurtoglu T, Basoglu H, Ozkisacik EA, et al. Effects of cilostazol on oxidative stress, systemic cytokine release, and spinal cord injury in a rat model of transient aortic occlusion. *Ann Vasc Surg*. 2014;28(2):479-488.
  38. Lee JH, Oh GT, Park SY, et al. Cilostazol reduces atherosclerosis by inhibition of superoxide and tumor necrosis factor- $\alpha$  formation in low-density lipoprotein receptor-null mice fed high cholesterol. *J Pharmacol Exp Ther*. 2005;313(2):502-509.
  39. Choi JM, Shin HK, Kim KY, Lee JH, Hong KW. Neuroprotective effect of cilostazol against focal cerebral ischemia via antiapoptotic action in rats. *J Pharmacol Exp Ther*. 2002;300(3):787-793.
  40. Hermes Tde A, Macedo AB, Fogaca AR, et al. Beneficial cilostazol therapeutic effects in mdx dystrophic skeletal muscle. *Clin Exp Pharmacol Physiol*. 2016;43(2):259-267.
  41. Torres LF, Duchon LW. The mutant mdx: inherited myopathy in the mouse. Morphological studies of nerves, muscles and end-plates. *Brain*. 1987;110(Pt 2):269-299.
  42. Whitehead NP, Pham C, Gervasio OL, Allen DG. N-acetylcysteine ameliorates skeletal muscle pathophysiology in mdx mice. *J Physiol*. 2008;586(7):2003-2014.
  43. Kido LA, Montico F, Sauce R, et al. Anti-inflammatory therapies in TRAMP mice: delay in PCa progression. *Endocr Relat Cancer*. 2016;23(4):235-250.
  44. Winterbourn CC, Hawkins RE, Brian M, Carrell RW. The estimation of red cell superoxide dismutase activity. *J Lab Clin Med*. 1975;85(2):337-341.
  45. Anderson BB, Carandina G, Lucci M, Perry GM, Vullo C. Red-cell GSH regeneration and glutathione reductase activity in G6PD variants in the Ferrara area. *Br J Haematol*. 1987;67(4):459-466.
  46. Yoshikawa T, Naito Y, Kishi A, et al. Role of active oxygen, lipid peroxidation, and antioxidants in the pathogenesis of gastric mucosal injury induced by indomethacin in rats. *Gut*. 1993;34(6):732-737.
  47. Carlberg I, Mannervik B. Glutathione reductase. *Methods Enzymol*. 1985;113:484-490.
  48. Wu CC, Bratton SB. Regulation of the intrinsic apoptosis pathway by reactive oxygen species. *Antioxid Redox Signal*. 2013;19(6):546-558.
  49. daSilva HNM, Covatti C, daRocha GL, et al. Oxidative stress, inflammation, and activators of mitochondrial biogenesis: tempol targets in the diaphragm muscle of exercise trained-mdx mice. *Front Physiol*. 2021;12:649793.
  50. Galluzzi L, Aaronson SA, Abrams J, et al. Guidelines for the use and interpretation of assays for monitoring cell death in higher eukaryotes. *Cell Death Differ*. 2009;16(8):1093-1107.
  51. Gunther C, He GW, Kremer AE, et al. The pseudokinase MLKL mediates programmed hepatocellular necrosis independently of RIPK3 during hepatitis. *J Clin Invest*. 2016;126(11):4346-4360.
  52. Cordani N, Pisa V, Pozzi L, Sciorati C, Clementi E. Nitric oxide controls fat deposition in dystrophic skeletal muscle by regulating fibro-adipogenic precursor differentiation. *Stem Cells*. 2014;32(4):874-885.
  53. Wang X, Zhao W, Ransohoff RM, Zhou L. Identification and function of fibrocytes in skeletal muscle injury repair and muscular dystrophy. *J Immunol*. 2016;197(12):4750-4761.
  54. Hermes TA, Mancio RD, Macedo AB, et al. Tempol treatment shows phenotype improvement in mdx mice. *PLoS One*. 2019;14(4):e0215590.
  55. Hermes TA, Mizobuti DS, daRocha GL, et al. Tempol improves redox status in mdx dystrophic diaphragm muscle. *Int J Exp Pathol*. 2020;101(6):289-297.
  56. Evans NP, Call JA, Bassaganya-Riera J, Robertson JL, Grange RW. Green tea extract decreases muscle pathology and NF- $\kappa$ B immunostaining in regenerating muscle fibers of mdx mice. *Clin Nutr*. 2010;29(3):391-398.
  57. Tonon E, Ferretti R, Shiratori JH, Santo Neto H, Marques MJ, Minatel E. Ascorbic acid protects the diaphragm muscle against myonecrosis in mdx mice. *Nutrition*. 2012;28(6):686-690.
  58. deSenzi Moraes Pinto R, Ferretti R, Moraes LH, Neto HS, Marques MJ, Minatel E. N-acetylcysteine treatment reduces TNF- $\alpha$  levels and myonecrosis in diaphragm muscle of mdx mice. *Clin Nutr*. 2013;32(3):472-475.
  59. Chattipakorn SC, Thummasorn S, Sanit J, Chattipakorn N. Phosphodiesterase-3 inhibitor (cilostazol) attenuates oxidative stress-induced mitochondrial dysfunction in the heart. *J Geriatr Cardiol*. 2014;11(2):151-157.

60. Burns DP, Ali I, Rieux C, Healy J, Jasione G, O'Halloran KD. Tempol supplementation restores diaphragm force and metabolic enzyme activities in mdx mice. *Antioxidants*. 2017;6(4):101.
61. Moraes LH, Bollineli RC, Mizobuti DS, Silveira Ldos R, Marques MJ, Minatel E. Effect of N-acetylcysteine plus deferoxamine on oxidative stress and inflammation in dystrophic muscle cells. *Redox Rep*. 2015;20(3):109-115.
62. Burns DP, Drummond SE, Bolger D, et al. N-acetylcysteine decreases fibrosis and increases force-generating capacity of mdx diaphragm. *Antioxidants*. 2019;8(12):581.
63. Buetler TM, Renard M, Offord EA, Schneider H, Ruegg UT. Green tea extract decreases muscle necrosis in mdx mice and protects against reactive oxygen species. *Am J Clin Nutr*. 2002;75(4):749-753.
64. Nakae Y, Hirasaka K, Goto J, et al. Subcutaneous injection, from birth, of epigallocatechin-3-gallate, a component of green tea, limits the onset of muscular dystrophy in mdx mice: a quantitative histological, immunohistochemical and electrophysiological study. *Histochem Cell Biol*. 2008;129(4):489-501.
65. Nakae Y, Dorchie OM, Stoward PJ, Zimmermann BF, Ritter C, Ruegg UT. Quantitative evaluation of the beneficial effects in the mdx mouse of epigallocatechin gallate, an antioxidant polyphenol from green tea. *Histochem Cell Biol*. 2012;137(6):811-827.
66. Grange RW, Isotani E, Lau KS, Kamm KE, Huang PL, Stull JT. Nitric oxide contributes to vascular smooth muscle relaxation in contracting fast-twitch muscles. *Physiol Genomics*. 2001;5(1):35-44.
67. Kaminski HJ, Andrade FH. Nitric oxide: biologic effects on muscle and role in muscle diseases. *Neuromuscul Disord*. 2001;11(6-7):517-524.
68. Loufrani L, Dubroca C, You D, et al. Absence of dystrophin in mice reduces NO-dependent vascular function and vascular density: total recovery after a treatment with the aminoglycoside gentamicin. *Arterioscler Thromb Vasc Biol*. 2004;24(4):671-676.
69. Asai A, Sahani N, Kaneki M, Ouchi Y, Martyn JA, Yasuhara SE. Primary role of functional ischemia, quantitative evidence for the two-hit mechanism, and phosphodiesterase-5 inhibitor therapy in mouse muscular dystrophy. *PLoS One*. 2007;2(8):e806.
70. Thomas GD, Ye J, De Nardi C, Monopoli A, Ongini E, Victor RG. Treatment with a nitric oxide-donating NSAID alleviates functional muscle ischemia in the mouse model of Duchenne muscular dystrophy. *PLoS One*. 2012;7(11):e49350.
71. Wu MY, Yiang GT, Liao WT, et al. Current mechanistic concepts in ischemia and reperfusion injury. *Cell Physiol Biochem*. 2018;46(4):1650-1667.
72. daMotta NA, deBrito FC. Cilostazol exerts antiplatelet and anti-inflammatory effects through AMPK activation and NF- $\kappa$ B inhibition on hypercholesterolemic rats. *Fundam Clin Pharmacol*. 2016;30(4):327-337.
73. Shi Q, Yin Z, Liu P, et al. Cilostazol suppresses IL-23 production in human dendritic cells via an AMPK-dependent pathway. *Cell Physiol Biochem*. 2016;40(3-4):499-508.
74. Aoki C, Hattori Y, Tomizawa A, Jojima T, Kasai K. Anti-inflammatory role of cilostazol in vascular smooth muscle cells in vitro and in vivo. *J Atheroscler Thromb*. 2010;17(5):503-509.
75. Carling D. AMPK signalling in health and disease. *Curr Opin Cell Biol*. 2017;45:31-37.
76. Palikaras K, Tavernarakis N. Mitochondrial homeostasis: the interplay between mitophagy and mitochondrial biogenesis. *Exp Gerontol*. 2014;56:182-188.
77. Mu J, Brozinick JT Jr, Valladares O, Bucan M, Birnbaum MJ. A role for AMP-activated protein kinase in contraction- and hypoxia-regulated glucose transport in skeletal muscle. *Mol Cell*. 2001;7(5):1085-1094.
78. Kim MJ, Lee JH, Park SY, et al. Protection from apoptotic cell death by cilostazol, phosphodiesterase type III inhibitor, via cAMP-dependent protein kinase activation. *Pharmacol Res*. 2006;54(4):261-267.
79. Disatnik MH, Dhawan J, Yu Y, et al. Evidence of oxidative stress in mdx mouse muscle: studies of the pre-necrotic state. *J Neurol Sci*. 1998;161(1):77-84.
80. Ljubcic V, Miura P, Burt M, et al. Chronic AMPK activation evokes the slow, oxidative myogenic program and triggers beneficial adaptations in mdx mouse skeletal muscle. *Hum Mol Genet*. 2011;20(17):3478-3493.
81. Abou-Samra M, Lecompte S, Schakman O, et al. Involvement of adiponectin in the pathogenesis of dystrophinopathy. *Skelet Muscle*. 2015;5:25.
82. Feng X, Li GZ, Wang S. Effects of estrogen on gastrocnemius muscle strain injury and regeneration in female rats. *Acta Pharmacol Sin*. 2004;25(11):1489-1494.
83. Huang J, Liu W, Doycheva DM, et al. Ghrelin attenuates oxidative stress and neuronal apoptosis via GHSR-1 $\alpha$ /AMPK/Sirt1/PGC-1 $\alpha$ /UCP2 pathway in a rat model of neonatal HIE. *Free Radic Biol Med*. 2019;141:322-337.
84. Fan Y, Yang Q, Yang Y, et al. Sirt6 suppresses high glucose-induced mitochondrial dysfunction and apoptosis in podocytes through AMPK activation. *Int J Biol Sci*. 2019;15(3):701-713.
85. Lee YJ, Shu MS, Kim JY, et al. Cilostazol protects hepatocytes against alcohol-induced apoptosis via activation of AMPK pathway. *PLoS One*. 2019;14(1):e0211415.

## SUPPORTING INFORMATION

Additional supporting information can be found online in the Supporting Information section at the end of this article.

**How to cite this article:** Hermes TdA, Mâncio RD, Mizobutti DS, et al. Cilostazol attenuates oxidative stress and apoptosis in the quadriceps muscle of the dystrophic mouse experimental model. *Int J Exp Path*. 2022;00:1-10. doi: [10.1111/iep.12461](https://doi.org/10.1111/iep.12461)